

Calorimetry with AI/ML for VBF Higgs to Invisible with ATLAS – and issues raised

Andrew Myers, Andy White (UTA)

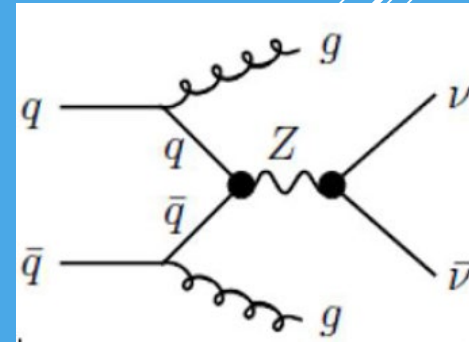
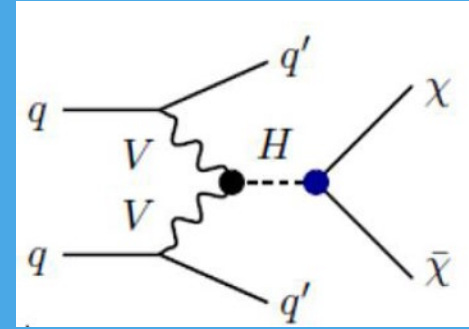
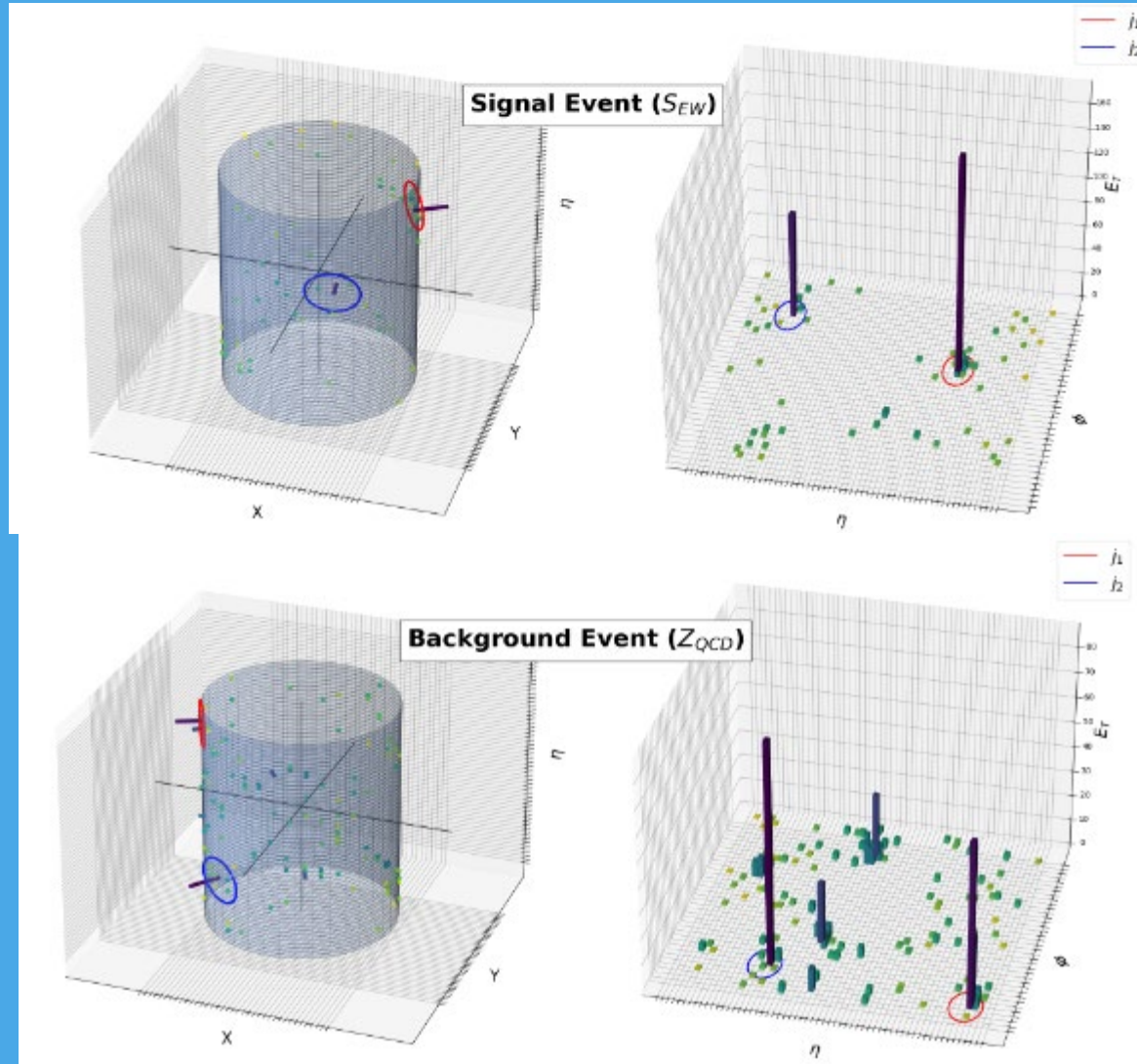


The current published ATLAS limit for $H \rightarrow$ invisible is 10.3%

Can we use AI/ML to get a better limit than cut based analysis?

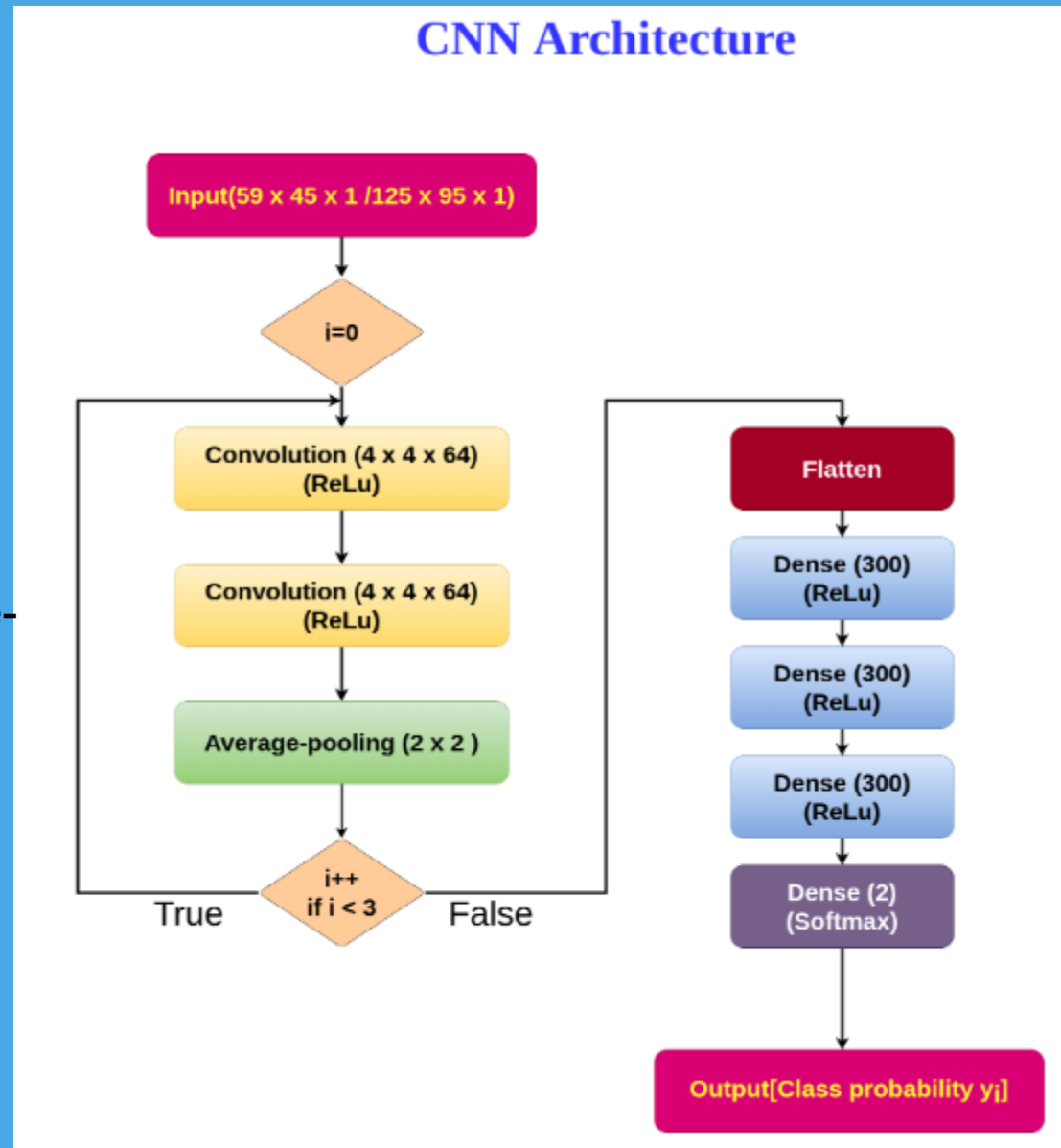
Machine learning analysis:

Calorimeter energy deposition patterns for Signal and Background



CNN is composed of three modules with each module formed by two convolutional layers followed by an average-pooling layer

arXiv:2008.05434v2 [hep-ph]
4 Nov 2020

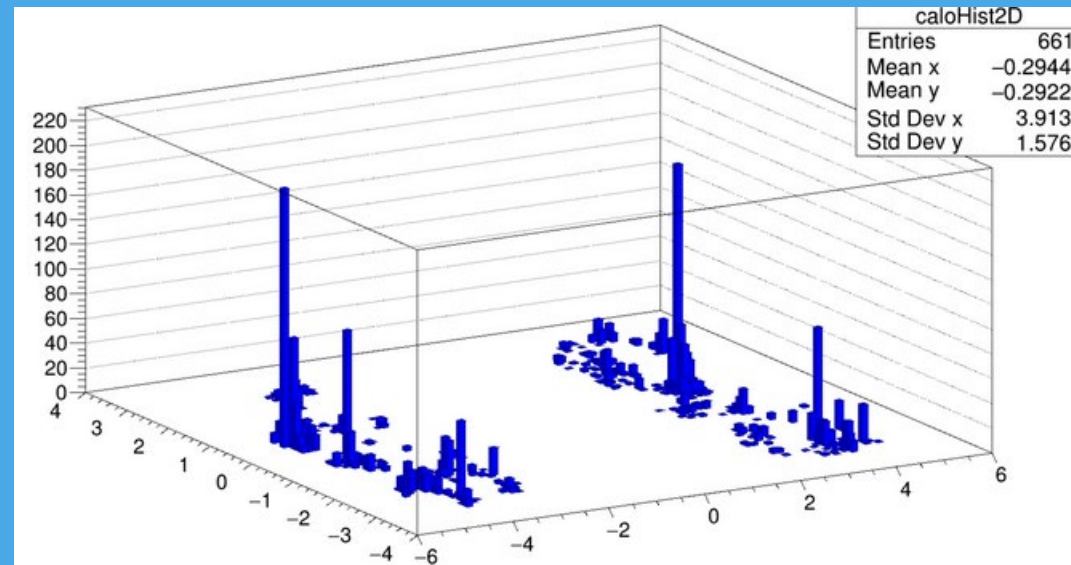


The third module's output is flattened and fed into a dense network of three layers having three hundred nodes each, which we pass into the final layer with the two nodes and softmax activation.

Level of Calorimeter Data for Input?

Options:

- Raw/calibrated calorimeter data - large volume, not easy to access, includes a lot of “noise” ?
- Calorimeter clusters – level of noise cut?
- “Noise” vs. low-level QCD activity (keep?)
- Topotowers – too “clean”?



Aspects of an “Intelligent Calorimeter

Can we/should we move intelligence into the calorimeter front end ?

Should we always propagate and save all the raw triggered data?

Should we use FE intelligence to e.g. “help” analyses by using AI to identify features?

Should we try to use AI to assist the trigger – can it be done?

Does AI mean we should rethink the whole TDAQ paradigm?

Sl.No	Name	Description	Expected median upper-limit on BR($h^0 \rightarrow \text{inv}$)		
			L = 36 fb ⁻¹	L = 140 fb ⁻¹	L = 300 fb ⁻¹
1.	$m_{jj}(\text{MET} > 250 \text{ GeV})$	reproduced shape analysis of reference [83]	$0.226^{+0.093}_{-0.063}$	$0.165^{+0.082}_{-0.056}$	$0.130^{+0.089}_{-0.027}$
2.	$ \Delta\eta_{jj} (\text{MET} > 250 \text{ GeV})$	$ \Delta\eta_{jj} $ analysis with shape-cuts of reference [83]	$0.200^{+0.080}_{-0.056}$	$0.128^{+0.050}_{-0.036}$	$0.106^{+0.041}_{-0.025}$
3.	$m_{jj}(\text{MET} > 200 \text{ GeV})$	m_{jj} shape analysis with weaker cut	$0.191^{+0.075}_{-0.053}$	$0.116^{+0.071}_{-0.036}$	$0.101^{+0.037}_{-0.045}$
4.	$ \Delta\eta_{jj} (\text{MET} > 200 \text{ GeV})$	$ \Delta\eta_{jj} $ analysis with weaker cut	$0.162^{+0.065}_{-0.045}$	$0.105^{+0.042}_{-0.029}$	$0.087^{+0.034}_{-0.025}$
5.	$\mathcal{P}_i^{LR}\text{-CNN}$	Low-Resolution, $\phi_0 = \phi_i$	$0.078^{+0.030}_{-0.022}$	$0.051^{+0.020}_{-0.014}$	$0.045^{+0.017}_{-0.012}$
6.	$\mathcal{P}_j^{HR}\text{-CNN}$	High-Resolution, $\phi_0 = \phi_{j_1}$	$0.070^{+0.027}_{-0.020}$	$0.043^{+0.017}_{-0.012}$	$0.035^{+0.013}_{-0.010}$
7.	$\mathcal{P}_{\text{MET}}^{LR}\text{-CNN}$	Low-Resolution, $\phi_0 = \phi_{\text{MET}}$	$0.092^{+0.037}_{-0.025}$	$0.062^{+0.024}_{-0.017}$	$0.053^{+0.023}_{-0.014}$
8.	$\mathcal{P}_{\text{MET}}^{HR}\text{-CNN}$	High-Resolution, $\phi_0 = \phi_{\text{MET}}$	$0.086^{+0.035}_{-0.024}$	$0.058^{+0.023}_{-0.016}$	$0.051^{+0.020}_{-0.014}$
9.	$\mathcal{K}\text{-ANN}$	8 kinematic-variables	$0.101^{+0.052}_{-0.022}$	$0.075^{+0.029}_{-0.021}$	$0.063^{+0.027}_{-0.017}$
10.	$\mathcal{R}\text{-ANN}$	16 radiative $H_T^{\eta C}$ variables	$0.138^{+0.055}_{-0.039}$	$0.094^{+0.036}_{-0.027}$	$0.079^{+0.032}_{-0.022}$
11.	$\mathcal{H}\text{-ANN}$	Combination of \mathcal{K} and \mathcal{R} variables	$0.094^{+0.038}_{-0.026}$	$0.065^{+0.026}_{-0.018}$	$0.057^{+0.022}_{-0.015}$

Table 1: Short description of the different analyses shown in figure 15 and the expected median upper-limit on BR($h^0 \rightarrow \text{inv}$) at 95% CL for each integrated luminosities which also include projections for L = 300fb⁻¹.